2010 International Conference on Nanotechnology and Biosensors
IPCBEE vol.2 (2011) © (2011) IACSIT Press, Singapore

Synthesis and Characterization of Nano-encapsulated Drug Delivery System for Bone Loss

Qingwen Ni[1,2]; Hong Dixon[1]
[1]Southwest Research Institute
San Antonio, TX, USA
[2]Texas A&M International University
Laredo, TX, USA
qni@swri.org; qni@tamiu.edu

Yi-Xian Qin
State University of New York at Stony Brook
Stony Brook
New York, USA

***Abstract*—A formulation of nano-encapsulated enantiomer of (+)promethazine with desired release rate has been synthesized for establish a localized drug delivery system. It was tested on a hind limb suspension (HLS) disuse rat model, and by using a non-destructive Nuclear Magnetic Resonance (NMR), and x-ray techniques to qualitatively evaluate the effectiveness of the new bone formations. Our studies suggest that nanoencapsulated (+)promethazine in controlled release formulations are effective in promoting bone growth in a rat model. Conjugating bone-targeting functional groups to the nanoparticles further enhances the efficacy of the drug.**

Keywords-nano-encapsulation, bone, NMR

I. INTRODUCTION

Bone loss, osteoporosis, is recognized as a significant major public health problems as well as in the space programs worldwide. Osteopenia is a disease characterized by long term loss of bone tissue, particularly in the weight-supporting skeleton [1-2]. Results of the joint Russian/US studies on the effect of microgravity on bone tissue from 4.5- to 14.5-month long missions have demonstrated that bone mineral density (BMD, g/cm^2) and mineral content (BMC, g) are diminished in all areas of the astronaut skeleton [3]. While osteopenia can affect the whole body, complications often occur predominantly at specific sites of the skeleton with great load bearing demands. The greatest BMD losses have been observed in the skeleton of the lower body, i.e., in pelvic bones (-11.99±1.22%) and in the femoral neck (-8.17±1.24%), while there was no apparent decay found in the skull region. On average, the magnitude and rate of the loss is staggering; astronauts lose bone mineral in the lower appendicular skeleton at a rate approaching 2% per *month* [4-5]. Similar results were found in the bed rest study. In a -6 degrees head-down tilt 7-day bed rest model for microgravity, it was observed that there was a decreased bone formation rate in the iliac crest [6]. To effectively countermeasure the bone loss, we need a better therapeutic system that can deliver the treatment in a need-base and non-invasively. An adequate understanding of the underlying mechanism and treatment strategy of such skeletal complications are extremely needed.

Most bone tissue turnover occurs at bone surfaces, such as at the interface to the marrow or in Haversian systems. Bone surfaces are normally covered by lining cells. In response to resorption stimuli these lining cells retract and expose the bone surface to attachment by osteoclasts and subsequent bone turnover. Therefore, targeting to the calcified matrix is most likely to occur at sites of active resorption. Bisphosphonates exhibit exceptionally high affinity to bone mineral hydroxyapatite; using a inactive bisphosphonate moiety deliver nanoencapsulated (+)promethazine provide a promising method to treat a variety of bone diseases [7-12]. Promethazine, an H_1 receptor blocker phenothiazine, was found to inhibit age-related bone loss in animal studies [13]; and the (+)enantiomer of promethazine was found to have a three fold higher efficacy for osteoclast inhibition than both the racemate and the (-)enantiomer [14].

It is known that Nuclear Magnetic Resonance (NMR) proton spin-spin (T_2) or spin-lattice (T_1) relaxation time measurements and analytical processing techniques have been used to determine microstructural characteristics of various types of fluid filled porous materials with characteristic pore sizes ranging from sub-micron to sub-millimeter [15-18]. Currently this method has been developed and applied to quantify in human cortical bone [19-23]. The observed proton NMR relaxation signals are a convolution of the relaxation of fluid in the pores throughout the observed system with the longer relaxation time corresponding to larger pore sizes.

The objective of this research study is to establish a unique localized drug delivery system for bone loss in the critical region by developing a nano-encapsulated medicine protocol to accelerate local therapeutic effects, and by using a non-invasive NMR relaxation technique, and other traditional methods (x-ray) to evaluate the effectiveness of the formation. In this program we have developed effective, less toxic nano-encapsulated drug, and control the release rate of nano-encapsulated formation to prevent bone loss by preparation of enantiomers of promethazine, and employ an animal (rat) disuse model to determine the efficacy of the bone-targeting micro-nanocapsule formulations of promethazine.

II. Material And Methods

A. Animal Model and Sample Population

A disuse animal model is developed through generated reduced or zero lower limb weight-bearing disuse hind limb suspension (HLS) rat model [24]. Rat femurs obtained from the Department of Biomedical Engineering, SUNY Stony Brook, New York through a collaborative relationship between SUNY and SwRI. HLS preparations were initially performed for two tests with 4 weeks for each test. First test by using formulated drug without targeting function on 30 female rats: 5 for disuse only, 5 for disuse with drug treated (encapsulation density/dosage), 5 for disuse+drug+30 min loading, 5 for disuse+drug+60 min loading, 5 for normal+drug, and 5 for normal. The adaptive responses were evaluated following four weeks period applied on 6 month old animals. Second test by using formulated drug with targeting function on 35 female rats: 5 for disuse only, 5 for disuse with drug (without targeting function) treated (encapsulation density/dosage), 5 for disuse with drug (with targeting function) treated (encapsulation density/dosage), 5 for disuse+drug+30 min loading, 5 for normal+drug (without targeting function) 5 for normal+drug (with targeting function), and 5 for normal. After first four weeks (drug without targeting function), and second four weeks (most of the drugs are with targeting function), the harvest cortical bone samples (right legs) were obtained from the rats. All the samples (right legs) were cleaned of soft tissues, and wrapped in calcium gauze and stored in separate containers filled with calcium buffered saline (CBS) and frozen at approximately -20^{o}C until testing.

B. NMR Determination

1) NMR Measurement

A Southwest Research Institute (SwRI) built 0.5 to 40 MHz broadline NMR system with an electromagnet of 19 inch diameter with a 4 inch gap was set up for a proton frequency of 27 MHz for these measurements. A laboratory-built 1.0 inch diameter rf coil was used in the experiment. ^{1}H spin-spin (T_2) relaxation profiles were obtained by using NMR CPMG [25-26]$\{90^0[-\tau - 180^0 - \tau\ (\text{echo})]_n - T_R\}$ spin echo method with a 6.5 μs wide 90^{o} pulse, τ of 500 μs, and T_R (sequences repetition rate) of 15 s. Each T_2 profile, one thousand echoes (one scan with n = 1000) were acquired and forty scans were used. Thus, one scan will have repeated 1000 echoes in the window. The data was measured on fresh frozen human femurs after complete thawing in the room temperature (21 ± 1^{o}C).

2) The Relationship Between NMR data and Effective Pore Sizes

Based on the low field NMR principle the diffusion effect may be negligible. Here, we accept the Brownstein and Tarr assumption [27] that the relaxation rate $1/T_2$ is proportional to the surface-to-volume (S/V) ratio of the pore

$$1/T2 = \rho\,(S/V)_{pore} \quad (1)$$

where ρ is the surface relaxivity, which is a measure of the effects of the pore surface enhancing the relaxation rate. Equation (1) indicates that the NMR relaxation time is proportional to pore size.

For a porous bone, the observed NMR magnetization will depend upon the T_2 of broad distributions of water in all pores. This implies that NMR transverse relaxation (T_2) data can be expressed as a sum of exponential functions:

$$M(t_i) = \sum_{j=1}^{m} f(T_{2,j})exp(-t_i/T_{2,j}) \quad (2)$$

where f ($T_{2,j}$)is proportional to the number of spins which relax with a time constant $T_{2,j}$. $M(t_i)$ is the NMR magnetization decay from fluid saturated cortical bone. Equation (2) can be inverted into a T_2 relaxation time distribution. Thus, instead of estimating a single relaxation time from a magnetization decay, it is necessary to estimate a inversion T_2 spectrum or distribution of relaxation time $f(T_{2,j})$, and an inversion relaxation technique was applied [15-16, 19, 20, 23]. Since T_2 depends linearly upon pore size, the T_2 distribution corresponds to pore-size distribution with the longer relaxation times having the larger pores. In addition, the median T_2 from the T_2 relaxation distribution can provide the overall effective bone pore size, i.e., the quality of whole bone. These results are also compared with x-ray data.

3) Median T2 Relaxation Time

The median T2 relaxation calculation is based on T_2 relaxation distribution data. In T_2 relaxation distribution spectra, the water intensity (amplitude in y axis) is plotted against T_2 relaxation time (x-axis) which corresponds to different pore sizes and the cumulative water intensity amplitudes, and is normalized to 1. Therefore, the middle point 0.5 on y axis corresponds to the median relaxation time on x-axis (Figure 3). This median relaxation time method can provide the whole relaxation mechanism without considering the bone size difference, i.e. different bone volume for different bone. It is also a sensitive method to analyze all pore size changes in an entire bone.

III. Results And Discussions

A. Synthesis of PLGA nanoparticles with encapsulated (+)promethazine

From our study the nanoparticles of (+)promethazine in block copolymers of poly (ethylene glycol)-b-poly(lactic acid glycolic acid) (PEG-PLGA) PLGA were successfully prepared with about 2% payload and an encapsulation efficiency of 40% by a double emulsion method. The nanoparticle size distributions are shown in Figure 1. The positively charged nanoparticle samples demonstrated controlled release of (+)promethazine for a day (Figure 2). The lyophilized nanoparticles can be re-suspended in pH7.4 PBS.

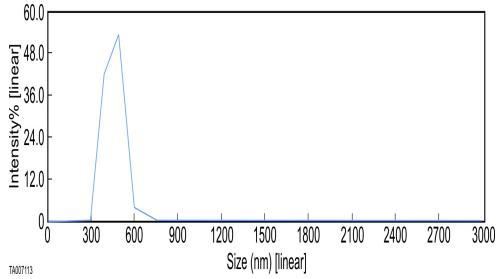

Figure 1. Particle size distribution of prepared (+) promethazine/PLGA nanoparticles

Particularly, the nanoparticles of (+)promethazine in PLGA-PEG block copolymers were successfully prepared by a double emulsion method. The results are similar to the ones obtained in Figure 1. PLGA-alendronate and PLGA-b-PEG copolymer nanoparticles with encapsulated (+)promethazine and nanoparticles of (+)promethazine/PLGA with bone-targeting moieties were prepared with alendronate conjugated PLGA polymers. The particle sizes of these samples were analyzed and they ranged between 50 and 200 nm. The zeta-potential and the payload of these samples were also analyzed by laser light scattering and HPLC respectively. Four nanoparticle samples were prepared for in vivo testing. The detailed sample properties can be found in Table 1 below.

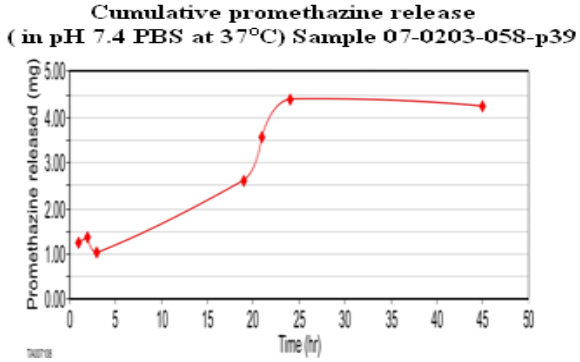

Figure 2. In vitro test for controlled release of nanoparticles of (+) promethazine.

B. *HLS Study #1: Formulated Drug without Target Function*

Figure 3 shows the examples of NMR median relaxation time, and T_2 relaxation distribution change for samples #131r (HLS + Drug). Figure 4 shows the comparison of T_2 distribution changes among samples HLS only, HLS + Drug, and control only after the volume normalization.

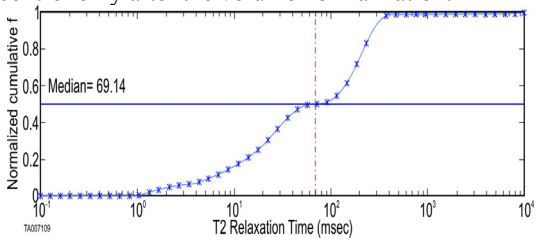

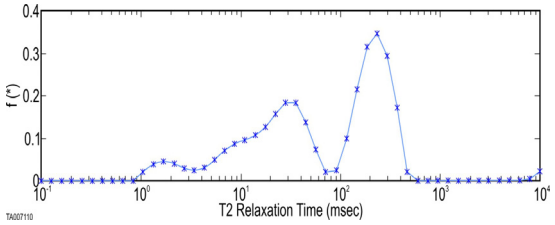

Figure 3. NMR relaxation time distribution (bottom) and median relaxation (top) for rat (right leg) after HLS only.

A summary of the median T2 relaxation time obtained from the in vivo animal studies (at HLS only, HLS+drug32A/32B, control + drug, and control only) is listed in Table 2, where the drug mixture of 32A/32B (without target function) was used. It is clear that on average, the drug32A/32B improves significantly over the disuse HLS. Meanwhile,drug 32A/32B had no effect on the control group.

In T_2 inversion relaxation spectra the longer relaxation time corresponds to larger pore sizes and the higher intensity corresponds to larger pore volume (Figure 4). Median relaxation time for HLS only (top one, sample # 126, ▲) is 69.11 ms; for HLS + drug (middle one, sample #, 132, ♦) is 52.88 ms; and for control (bottom one, sample # 155, ●) is 43.80 ms. This NMR data are consistent with the X-ray data shown in Figure 5.

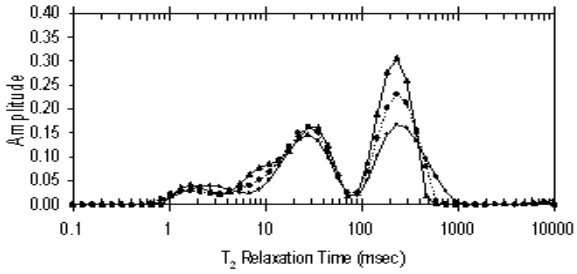

Figure 4. The comparison of T_2 distribution changes among the samples of HLS only (high pesk,▲), HLS+drug (median peak, ♦), and control only (low peak, ●), after the volume normalization.

C. *HLS Study #2: Formulated Drug with Target Function*

A summary of the median T_2 relaxation times obtained from the animal studies (at HLS only, HLS+drug33A/33B, control + drug33A/33B, and control only) is listed in Table 3, where the drug mixture of 33A/33B (with targeting function) was used. Although there was some data

Figure 5. X - ray data for rats at HLS only, HLS + drug32A/23B, and HLS + drug32A/32B+force loading (left to right).

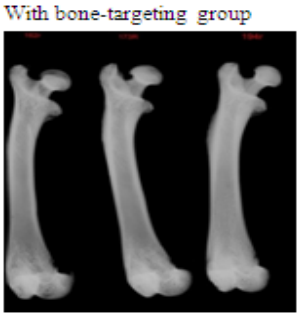

Figure 6. X - ray data for samples of HLS only, HLS + drug33A/33B, and control only (left to right).

scattering, it is apparent that on average, the mixture of drug33A/33B demonstrated improvement over 32A/32B (without targeting function). And drug 33A/33B had no effect on the control group.

IV. Conclusions

From our study the promising formulations and test results were obtained such as 1) PLGA-b-PEG copolymer encapsulated (+)promethazine; 2) PLGA-alendronate copolymer encapsulated (+)promethazine; and 3) controlled release of (+)promethazine from the nanoparticles formulations when tested in vitro; and 4) the nanoparticles with encapsulated (+)promethazine drug showed significant bone-density improvement for the rats in a HLS (in vivo) test, and the formulation with the target function showed further improvement. Further studies are planned it includes comparing our unique drug with a commercial drug alendronate and utilizing a inactive bisphosphonate as a targeting group, establishing efficacy of the unique localized drug delivery system to prevent bone loss. The formulations may show significant improvement for bone loss in humans as well.

Acknowledgments

This work is supported by Southwest Research Institute (SwRI) project R9742. We thank Dr. S. Chen's lab for doing x-ray measurements for us.

Reference

[1] B. L. Riggs and L. J. Melton, III. The prevention and treatment of osteoporosis. N.Engl.J.Med. 327:620-627,8-27-1992.

[2] B. L. Riggs and L. J. Melton, III. The worldwide problem of osteoporosis: insights afforded by epidemiology. Bone. 17:505S-511S,1995.

[3] A. I. Grigoriev, V. S. Oganov, A. V. Bakulin, V. V. Poliakov, L. I. Voronin, V. V. Morgun, V. S. Shnaider, L. V. Murashko, V. E. Novikov, A. LeBlanc, and L. Shackelford. Clinical and Psychological Evaluation of Bone Changes Among Astronauts after Long Term Space Flights (Russian). Aviakosmicheskaia I Ekologicheskaia Meditsina. 32:21-25,1998.

[4] A. LeBlanc, V. Schneider, and L. Shackelford. Bone Mineral and Lean Tissue Loss after Long Duration Spaceflight. Trans.Amer.Soc.Bone Min.Res. 11S:567-1996.

[5] A. LeBlanc, L. Shackelford, A. Feiveson, and V. Oganov. Bone Loss in Space: Shuttle/Mir Experience and Bed-Rest Counter Measure Program. 1:17-1999.

[6] S. B. Arnaud. J. S. Harper, and M. Navidi. Mineral distribution in rat skeletons after exposure to a microgravity model.J.Gravit.Physiol. 2:115-116,1995.

[7] H. Uludag, T. Gao, G. R. Wohl, D. Kantoci, and R. F. Zernicke. Bone affinity of a bisphosphonate-conjugated protein in vivo. Biotechnol.Prog. 16:1115-1118,2000.

[8] H. Uludag and J. Yang. Targeting systemically administered proteins to bone by bisphosphonate conjugation. Biotechnol.Prog. 18:604-611,2002.

[9] J. E. Wright, L. Zhao, P. Choi, and H. Uludag. Simulating hydroxyapatite binding of bone-seeking bisphosphonates. Adv.Exp.Med.Biol. 553:139-148,2004.

[10] S.A. Gittens, G. Bansal, C. Kucharski, M. Borden, and H. Uludag. Imparting mineral affinity to fetuin by bisphosphonate conjugation: a comparison of three bisphosphonate conjugation schemes. Mol.Pharm. 2:392-406,2005

[11] S. Zhang, J. E. Wright, G. Bansal, P. Cho, and H. Uludag. Cleavage of disulfide-linked fetuin-bisphosphonate conjugates with three physiological thiols. Biomacromolecules. 6:2800-2808,2005.

[12] J. E. Wright, S. A. Gittens, G. Bansal, P. I. Kitov, D. Sindrey, C. Kucharski, and H. Uludag. A comparison of mineral affinity of bisphosphonate-protein conjugates constructed with disulfide and thioether linkages. Biomaterials. 27:769-784,2006.

[13] T.J. Hall, H. Nyugen, M. Schaeublin, M. Michalsky, and M. Missbach. Phenothiazines are potent inhibitors of osteoclastic bone resorption. Gen.Pharmacol. 27:845-848,1996.

[14] E. J. Boland, US patent application 2006/0258650 A1. Phenothiazine enantiomers as agents for the prevention of bone loss.2006

[15] D. P. Gallegos, Munn, K., Smith, D. M., and Stermer, D. L. A NMR Technique for the Analysis of Pore Structure: Application to Materials with Well-Defined Pore Structure, J. Colloid Interface Sci 119 127.1987

[16] C.L.Glaves and Smith D.M. Membrane Pore Structure Analysis Via NMR Spin-Lattice Relaxation Experiments, J. Member. Sci. 46 167. 1989

[17] M.M. Chui, Philips, R.J., and McCarthy, M.Measurement of the Porous Microstructure of Hydrogels by Nuclear Magnetic Resonance, J. Colloid Interface Sci. 174 336.1995

[18] W. E. Kenyon. Petrophysical Principles of Applications of NMR Logging, The Log Analyst, Mar.-Apr. 21.1997

[19] X. Wang, and Ni, Q. 2003. Determination of Cortical Bone Porosity and Pore size Distribution Using a Field NMR Approach, J. Orthop. Res. 21(2): 312-319.

[20] Q. Ni, King, J.D. and Wang, X.Characterization of Human Bone Structure Changes By Low Field NMR, Measurement Science and Technology, 15, 58 – 66. 2004.

[21] P. Fantazzini, Bortolotti, V., Brown, R.J.S., Garavaglia, C., Viola, R., Giavaresi, G.Two 1H-nuclear magnetic resonance methods to measure internal porosity of bone trabeculae: By solid-liquid signal separation and by longitudinal relaxation. Journal of Applied Physics Vol 95, 339-343. 2004.

[22] Q. Ni, and Nicolella, D.P. The Characterization of Human Cortical Bone Microdamage by Nuclear Magnetic Resonance. Measurement Science and Technology, 16, 659-668.2005

[23] Q. Ni, Nyman, J., Wang, X., De Los Santos, A. and Nicolella, D.Assessment of Water Distribution Changes in Human Cortical Bones by Nuclear Magnetic Resonance. Measurement Science and Technology, 18, 715-723.2007

[24] E. R. Morey-Holton, B. P. Halloran, L. P. Garetto, and S. B. Doty. Animal housing influences the response of bone to spaceflight in juvenile rats. J.Appl.Physiol. 88:1303-1309,2000

[25] H.Y. Carr, and Purcell, E. M. Effects of Diffusion on Free Precession in Nuclear Magnetic Resonance Experiments. Phys. Rev. 904, No.3 630. 1954

[26] S. Meiboom, and Gill, D. Modified Spin-Echo Method for Measuring Nuclear Relaxation Times. Rev. Sci. Inst. 29, 688. 1958

[27] K.R. Broenstein and C.E. Tarr. Importance of Classical Difussion in NMR Studies of Water in Biological Cells. Phys Rev. A 19, 2446, 1979.

TABLE I. DETAILS OF THE NANOPARTICLE SAMPLES USED IN THE ANIMAL STUDY.

Sample No.	Composition	(+) Promethazine.HCl Payload (%, by HPLC)	Zeta potential (mV)
08-0203-011-p32A	10 mg (+) promethazine.HCl 300 mg 5%PEG-PLGA	29.1	-38
08-0203-011-p32B	10 mg (+) promethazine.HCl 300 mg 10%PEG-PLGA	13.0	-32
08-0203-011-p33A	10 mg (+) promethazine.HCl 200 mg 5%PEG-PLGA 100 mg PLGA-alendronate (target function)	14.9	-51
08-0203-011-p33B	10 mg (+) promethazine.HCl 200 mg 10%PEG-PLGA 100 mg PLGA-alendronate (target function)	19.0	-38

TABLE II. MEDIAN RELAXATION TIMES ARE LISTED FOR DIFFERENT GROUP SAMPLES WHERE DRUG IS WITHOUT TARGET FUNCTION.

Sample # (HLS)	Median relaxation (ms)	Sample # (HLS+drug32 A/32B)	Median relaxation (ms)	Sample # (Control+drug32 A/32B)	Median relaxation (ms)	Sample # (Control only)	Median relaxation (ms)
126	69.11	131	50.54	146	39.69	151	41.30
127	49.65	132	52.80	147	48.72	152	41.32
128	75.66	133	52.88	148	39.70	153	36.50
129	67.77	134	57.28	149	51.43	154	58.65
130	51.24	135	45.12	150	50.20	155	43.85
Average	62.69±11.58	Average	51.72±4.43	Average	45.95±7.79	Average	44.32±4.39

TABLE III. MEDIAN RELAXATION TIMES ARE LISTED FOR DIFFERENT GROUP SAMPLES WHERE DRUG IS WITH TARGET FUNCTION.

Sample # (HLS)	Median relaxation (ms)	Sample # (HLS+drug 33A/33B mixture)	Median relaxation (ms)	Sample # (Control+drug33 A/33B mixture)	Median relaxation (ms)	Sample # (Control only)	Median relaxation (ms)
161	76.38	173	44.92	181	42.84	191	48.93
162	67.88	175	47.07	182	44.40	192	47.90
163	74.66	176	37.24	183	46.83	193	38.74
170	51.26	177	44.05	184	42.06	194	40.86
172	40.62	179	59.39	185	39.88	195	39.56
Average	62.16±15.6	Average	46.53±8.07	Average	43.21±2.60	Average	43.20±4.84